Magnetar superconductivity versus magnetism: Neutrino cooling processes

Monika Sinha* and Armen Sedrakian
Institute for Theoretical Physics, J. W. Goethe-University, D-60438 Frankfurt am Main, Germany
(Received 24 November 2014; revised manuscript received 29 January 2015; published 30 March 2015)

We describe the microphysics, phenomenology, and astrophysical implication of a B-field induced unpairing effect that may occur in magnetars, if the local B field in the core of a magnetar exceeds a critical value H_{c2}. Using the Ginzburg-Landau theory of superconductivity, we derive the H_{c2} field for proton condensate taking into the correction ($\leqslant$30%) which arises from its coupling to the background neutron condensate. The density dependence of pairing of proton condensate implies that H_{c2} is maximal at the crust-core interface and decreases towards the center of the star. As a consequence, magnetar cores with homogenous constant fields will be partially superconducting for "medium-field" magnetars ($10^{15} \leqslant B \leqslant 5 \times 10^{16}$ G) whereas "strong-field" magnetars ($B > 5 \times 10^{16}$ G) will be void of superconductivity. The neutrino emissivity of a magnetar's core changes in a twofold manner: (i) the B-field assisted direct Urca process is enhanced by orders of magnitude, because of the unpairing effect in regions where $B \geqslant H_{c2}$; (ii) the Cooper-pair breaking processes on protons vanish in these regions and the overall emissivity by the pair-breaking processes is reduced by a factor of only a few.

DOI: 10.1103/PhysRevC.91.035805 PACS number(s): 97.60.Jd, 26.60.−c, 95.85.Sz, 74.20.De

I. INTRODUCTION

The protonic fluid in the cores of magnetized neutron stars is a type-II superconductor, i.e., it supports the magnetic B field by forming quantized electromagnetic vortices with density $n_v = B/\Phi_0$, where $\Phi_0 = \pi\hbar c/e$ is the quantum of flux, in the field range $H_{c1} \leqslant B \leqslant H_{c2}$ [1]. The lower critical field H_{c1} is the field strength at which the emergence of the first vortex (flux tube) becomes energetically favorable. At the upper critical field strength H_{c2} the normal cores of the vortices touch each other and superconductivity is destroyed. The H_{c2} field is density-dependent and is given by

$$H_{c2} = \frac{\Phi_0}{2\pi\xi_p^2}, \tag{1}$$

where ξ_p is the coherence length of the proton condensate, which scales inversely with the pairing gap Δ. The coherence length appears in Eq. (1) because H_{c2} is the field at which the Larmor radius of protons becomes comparable to the size of a Cooper pair $\sim\xi_p$. A field $B \sim H_{c2}$ disrupts the coherence among the protons which form a Cooper pair and, therefore, destroys their superconductivity. For the proton superconductor in the cores of neutron stars $10^{15} \leqslant H_{c2} \leqslant 10^{17}$ G, i.e., H_{c2} is well above the fields expected in the interiors of ordinary neutron stars ($B \sim 10^{12}$–10^{13} G).

The inferred magnetic fields on the surfaces of magnetars are of the order of 10^{15} G. Their interior B fields are not known, but it has been frequently conjectured that they are larger than the surface field. The conjectured maximal B field, which is consistent with the virial theorem for self-gravitating magnetic equilibria, is of the order $B_{\max} \simeq 10^{18}$ G. Because $B_{\max} > H_{c2}$ and because these fields may vary over the star's core, we may anticipate an intimate interplay between the magnetism and superconductivity in the interiors of magnetars depending on whether the local field is above or below H_{c2}. Some observational arguments where put forward in recent years in favor of type-I superconductivity [2,3]. However, our choice of the equations of state of dense matter and microscopic parameters of the proton superconductor predict type-II superconductivity throughout most of the core of a neutron star, as we show below.

The purpose of this work is to show that large enough magnetic fields in the interiors of magnetars unpair proton superconductor in a strongly density-dependent manner. We then go on to study the consequences of this magnetically induced unpairing effect on the neutrino emissivity of magnetars. Neutrino emissivities are the key ingredients for the simulations of thermal evolution of magnetars and can be confronted with the measured x-ray fluxes from the surfaces of magnetars.

This paper is structured as follows. In Sec. II we discuss the input physics, i.e., the underlying equation of state (EoS) and composition of matter which sets the stage for the following discussion. In Sec. III, starting from the Ginzburg-Landau (GL) functional for proton superconductor coupled to neutron superfluid, we derive an expression H_{c2}, which accounts for the density-density coupling between the proton and neutron condensates. In Sec. IV we compute the neutrino emissivities of the Urca process and pair-breaking processes in magnetars including the unpairing effect. Our conclusions and an outlook are given in Sec. V.

II. MICROPHYSICAL INPUT

Consider a magnetar with a nonstrange baryonic core consisting of neutrons (n), protons (p), electrons (e), and muons (μ) in β equilibrium. We choose to work with a relativistic density functional (DF) with density-dependent couplings derived in Ref. [4] to obtain the equation of state (EoS) and composition of matter in the star's core and inner crust.

*Present address: Indian Institute of Technology Rajasthan, Old Residency Road, Ratanada, Jodhpur 342011, India.

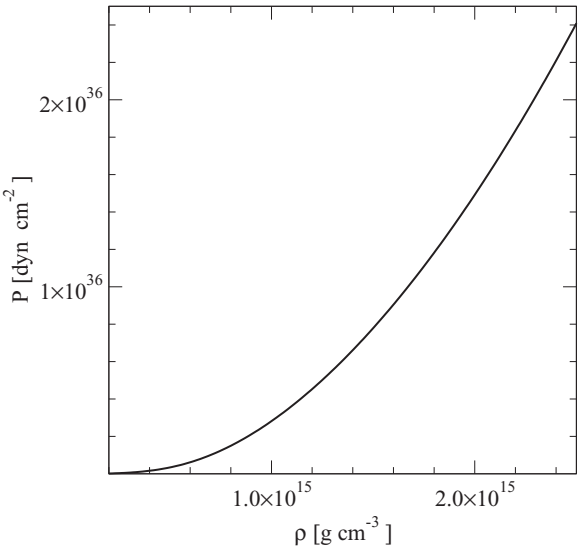

FIG. 1. Zero-temperature equation of state of dense matter composed of neutrons, protons, electrons, and muons in β equilibrium derived from the relativistic DF with the parametrization of Ref. [4].

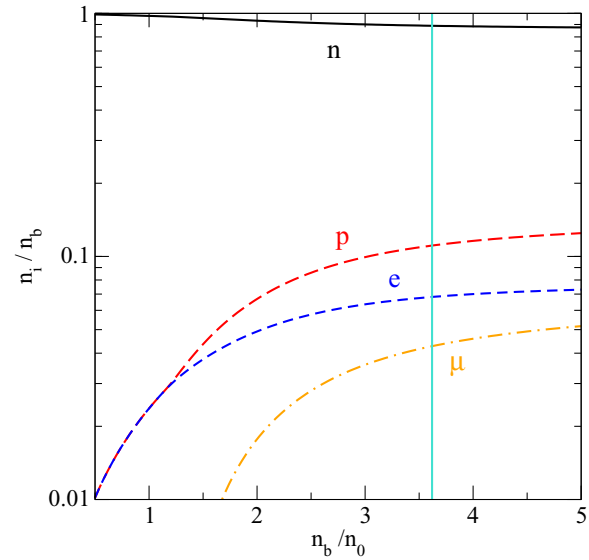

FIG. 2. (Color online) Dependence of particle abundances n_i/n_b, $i \in n,p,e,\mu$ on the net baryon density n_b in units of saturation density $n_0 = 0.152$ fm^{-3}. The vertical line shows the approximate Urca threshold $Y_{\rm Urca} = 0.11$ for proton fraction.

The latter parametrization is in excellent agreement with the nuclear phenomenology as it predicts saturation density $n_0 = 0.152$ fm^{-3}, binding energy per nucleon $E/A = -16.14$ MeV, incompressibility $K_0 = 250.90$ MeV, symmetry energy $J = 32.30$ MeV, symmetry energy slope $L = 51.24$ MeV, and symmetry incompressibility $K_{\rm sym} = -87.19$ MeV all taken at saturation density [5]. For completeness we show the EoS of baryonic matter in Fig. 1 derived from this DF. Compact star models based on this DF were constructed elsewhere [6] where it has been shown that the resulting maximum mass predicted by this EoS is well above the current observational lower limit $2M_\odot$ on the maximum mass of any compact star. Strangeness in form of hyperons or deconfined two- or three-flavor quark matter may appear in the centers of magnetars, but we neglect this possibility in the following.

The composition of dense matter corresponding to our EoS is shown in Fig. 2, where we show the abundances of species n_i/n_b, where $i \in n,p,e,\mu$ as a function of baryon density n_b normalized by the nuclear saturation density of the DF. The abundances of protons and electrons are equal up to the point where muons set in. The threshold value of Urca process in nonmagnetized matter $n_p/n_b \sim 0.11$ is reached at the density $n \simeq 3n_0$. The composition of matter itself will be affected by a strong B field, when electromagnetic interactions become of the order of the nuclear scale set by the Fermi energies of the constituents. However, below the field values 10^{18} G the abundances of baryons for nonzero B are indistinguishable from those in the $B = 0$ case (see Ref. [7] and references therein).

The pairing channels in neutron star matter correspond to the attractive most dominant phase-shifts at given density or energy of nucleons (for a review see, e.g., Ref. [8]). Low density neutron matter in the crust of compact stars pairs in the $^1S_0$ channel; above the saturation density the neutron fraction is large enough (and energies are high enough) to render the S-wave interaction repulsive. The dominant pairing at these densities is in the $^3P_2$-$^3F_2$ channel. Protons are in the continuum in the fluid core of the star and are much less abundant than neutrons, therefore their energies are low enough to favor the $^1S_0$ pairing. The pairing gaps in these dominant channels adopted from Refs. [9] are shown in Fig. 3. The formulas which fit these gaps are listed in the Appendix. At asymptotically high densities pairing of protons in the $^3P_2$-$^3F_2$ channel may occur. In the exceptional models

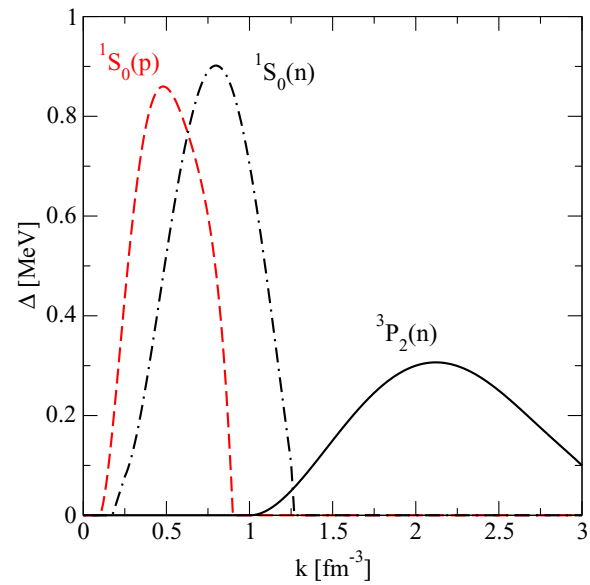

FIG. 3. (Color online) Dependence of S- and P-wave pairing gaps of neutrons (dash-dotted and solid lines) and of S-wave protons (dashed line) on their respective Fermi momenta.

where matter is nearly isospin symmetrical at high densities, spin-one, isospin-zero pairing in the $^3D_2$ channel may become the dominant one [10]. Examples of such models are those which feature kaon condensates. Below we do not consider proton P-wave pairing or neutron-proton D-wave pairing.

III. GINZBURG-LANDAU THEORY OF H_{c2} IN DENSE MATTER

Type-II superconductivity is characterized by the GL parameter, $\kappa = \delta_L/\xi_p$, where δ_L is the London penetration depth of the B field in a superconductor, having the range

$$\frac{1}{\sqrt{2}} < \kappa < \infty. \tag{2}$$

The critical value $\kappa_c = 1/\sqrt{2} = 0.7071$ separates the domains of type-I and type-II superconductivity.

The magnetic field is confined to electromagnetic vortices for field values between the lower H_{c1} and upper H_{c2} critical fields. If the B field is lager than H_{c2} it unpairs the Cooper pairs and the material makes a transition to the normal state. The phase transition from superconducting to the normal state in the vicinity of H_{c2} can be described in terms of the GL theory, because the superconducting order parameter is small. Note that in the vicinity of H_{c2} the superconducting order parameter is small because of the large B field and the GL expansion is valid not only near the critical temperature T_c, but in the entire temperature range $0 \leqslant T \leqslant T_c$.

We start by writing down the GL functional for a superfluid neutron and superconducting proton mixture

$$F[\phi,\psi] = F_n[\phi] + \alpha\tau|\psi|^2 + \frac{b}{2}|\psi|^4 + b'|\psi|^2|\phi|^2 + \frac{1}{4m_p}\left|\left(-i\hbar\nabla - \frac{2e}{c}\boldsymbol{A}\right)\psi\right|^2 + \frac{B^2}{8\pi}, \tag{3}$$

where ψ and ϕ are the proton and neutron condensate wave functions, m_p is the proton mass, $\tau = (T - T_{cp})/T_{cp}$, where T_{cp} is the critical temperature of superconducting phase transition of protons. Here α and b are the coefficients of the GL expansion for the proton condensate, b' describes the density-density coupling between the neutron and proton condensates. This type of GL functional was analyzed initially to study the current-current coupling between the neutron and proton condensates [11] (the entrainment effect, see Ref. [12]). More recent study of Ref. [3] discusses the density-density coupling between the neutron and proton condensates and provides the relevant microscopic expressions for the coefficient of the GL functional. The effective vector potential can be decomposed as $\boldsymbol{A} = \boldsymbol{A}_{\rm em} + \boldsymbol{A}_{\rm ent}$, where the first term is the ordinary vector potential of electromagnetism with $\boldsymbol{B} = \nabla \times \boldsymbol{A}$. The second term is the "entrainment" vector potential $\boldsymbol{A}_{\rm ent} = (\hbar c/e)[(m_p^* - m_p)/m_p]\nabla\phi$, where m_p^* is the proton effective mass, see Ref. [11]. The entrainment effect describes the current-current coupling between the neutron and proton condensates. The explicit form of the contribution of the neutron condensate to the GL functional, $F_n[\phi]$, is not required in the following.

The minimization of the GL functional with respect to ψ^*, i.e., $\delta F[\phi,\psi]/\delta\psi^* = 0$ gives

$$\frac{1}{4m_p}\left(-i\hbar\nabla - \frac{2e}{c}\boldsymbol{A}\right)^2\psi + \alpha\tau\psi + b|\psi|^2\psi + b'|\phi|^2\psi = 0. \tag{4}$$

The equilibrium value of the condensate is given by the solution of Eq. (4)

$$\psi(\alpha\tau + b|\psi|^2 + b'|\phi|^2) = 0, \tag{5}$$

from which we obtain the two possible equilibrium solutions

$$\psi = 0, \quad T > T_c, \tag{6}$$

$$|\psi|^2 = -\frac{1}{b}(\alpha\tau + b'|\phi|^2), \quad T \leqslant T_c. \tag{7}$$

The variation of the GL functional with respect to the electromagnetic vector potential $\delta F[\phi,\psi]/\delta\boldsymbol{A} = 0$ gives

$$\frac{c}{4\pi}\nabla \times \nabla \times \boldsymbol{A} = \boldsymbol{j}, \tag{8}$$

where

$$\boldsymbol{j} = -\frac{i\hbar e}{m}(\psi^*\nabla\psi - \psi\nabla\psi^*) - \frac{4e^2}{mc}|\psi|^2(\boldsymbol{A}_{\rm em} + 2\boldsymbol{A}_{\rm ent}) \tag{9}$$

is the proton supercurrent. It contains the conventional electromagnetic current $\propto\nabla\psi$ as well as the entrainment current $\propto\boldsymbol{A}_{\rm ent} \propto \nabla\phi$.

Equations (4), (8), and (9) constitute the GL equations in their most general form. To derive the value of the upper critical field H_{c2} it is sufficient to keep only the linear in ψ terms in the GL equations above. To this order Eq. (9) reduces to

$$\nabla \times \nabla \times \boldsymbol{A} = 0 + O(|\psi|^2). \tag{10}$$

Furthermore, because $\nabla \times \boldsymbol{A}_{\rm ent} = 0$ identically (except at the singular points where the neutron vortices are located), we can make the replacement $\boldsymbol{A} \to \boldsymbol{A}_{\rm em}$ in Eq. (10). The small-scale (local) magnetic field is homogenous, therefore the corresponding vector potential $\boldsymbol{A}_{\rm em}$ is linear in coordinates. We choose $\boldsymbol{A}_{\rm em}$ along one of the directions of the Cartesian system of coordinates, say z direction, without loss of generality. Assume that the B field is in the y direction. Then, $\psi = \psi(x)$ only. To linear order in ψ the solution of Eq. (5) is $A_{\rm em} = Bx$. Substituting this into the first GL equation (4) one finds

$$-\psi'' + \frac{4\pi^2}{\Phi_0^2}B^2x^2\psi = -\frac{4m_p}{\hbar^2}(\alpha\tau + b'|\phi|^2)\psi + O(|\psi|^2). \tag{11}$$

The mathematical form of this equation is that of the harmonic oscillator, therefore, its solutions is read off as

$$-\frac{4m_p}{\hbar^2}(\alpha\tau + b'|\phi|^2) = \left(n + \frac{1}{2}\right)\frac{4\pi B}{\Phi_0}. \tag{12}$$

We are interested in the strongest field for which solutions with $\psi \neq 0$ are still possible. This is the case $n = 0$ in Eq. (12)

which identifies the critical field $B = H_{c2}$. Consequently

$$H_{c2} = \frac{\Phi_0}{2\pi}\left[-\frac{4m_p}{\hbar^2}(\alpha\tau + b'|\phi|^2)\right] = \frac{\Phi_0}{2\pi\xi_p^2}\left[1 + \frac{|b'||\phi|^2}{\alpha|\tau|}\right], \quad (13)$$

where we used the relation $(m_p|\alpha\tau|)^{1/2} = \hbar/2\xi_p$ and the fact that $b' < 0$, see below. If $b' = 0$ Eq. (13) reduces to the standard result [13]. To evaluate the correction to the critical field note that $|\alpha\tau| = |\psi_0|^2 b$ and, therefore, $(b'|\phi|^2/\alpha\tau) = (n_n/n_p)(|b'|/|b|)$.

The coefficient b' which takes into account beyond mean-field coupling between the neutron and proton condensates was computed by Alford *et al.* [3] in β-equilibrated, charge-neutral nuclear matter diagrammatically. They also provide the mean-field expression for b. Using their results we find that

$$\frac{n_n}{n_p}\frac{|b'|}{|b|} = \frac{27\pi^2}{4}G_{np}\frac{n_n^2}{\mu_p^2\mu_n^2}\frac{\Delta_p^2}{m_p k_{F_p}}, \quad (14)$$

where we used the value of b' valid in the regime $\Delta_p \ll \mu_p$ and $\Delta_n \ll \mu_n$ and $T \to 0$ and the value of parameter $G_{np} = 10^{-5}$ MeV^{-2} [3]. Note that close to the critical temperature T_c alternative expressions provided by Alford *et al.* [3] should be used. The correction in Eq. (13) owing to the coupling between the neutron and proton condensates is $\leqslant 30\%$; it is small because the coupling between the condensates arises only via fluctuations which vanish in the ground state. The main uncertainty in Eq. (14) is the contact pairing interaction in the isosinglet channel G_{np}; its value quoted above should be viewed as an order of magnitude estimate. An additional uncertainty arises from the not well-known value of the gap in the proton spectrum Δ_p which may vary by a factor of few.

The analogy between Eq. (11) and the one describing harmonic oscillator in quantum mechanics can be exploited further to write down the most-general "harmonic oscillator" type solution of Eq. (11), which describes a vortex in the x-y plane (with the field directed in the z direction). The corresponding wave function can be written as

$$\psi(x,y) = \sum_{n=-\infty}^{\infty} C_n \exp[-\kappa B(x - k/\kappa B)^2/2 + iky], \quad (15)$$

where the coefficient C_n and k depend on the type of the proton vortex lattice. Assuming triangular lattice one finds $k = \kappa(\pi\sqrt{3})^{1/2}$ and the set of conditions $C_{n+4} = C_n$, $C_0 = C_1 = C$, $C_2 = C_3 = -C$, where C is given by the normalization of the wave function to the density of condensate.

Table I lists the key parameters of the proton superconductor for a range of densities corresponding to the star's fluid core. The coherence length has a minimum, which reflects the density dependence of the gap ($\xi_p \propto \Delta^{-2}$). Because H_{c2} scales inversely with ξ_p^2, the critical field has a maximum, with max $H_{c2} = 7.37 \times 10^{16}$ G at $n_b = 0.7 n_0$ in our setup. The London penetration depth scales as the root of inverse proton density, therefore it decreases as the density increases. This has the consequence that the GL parameter drops below the critical value κ_c and the proton superconductor becomes type-I. However, this occurs only in the high-density end of the proton superconductivity domain and should be relevant only for compact stars with central densities exceeding this value.

TABLE I. Microscopic parameters of proton superconductor and the upper critical field for unpairing H_{c2} for a range of matter densities.

n_b/n_0	k_{Fp}	Δ_p	m_p^*/m_p	ξ_p	δ_L	κ	H_{c2}
0.140	0.12	0.02	0.93	76.1	929.2	12.2	0.06
0.300	0.20	0.24	0.89	11.9	425.0	35.6	3.15
0.500	0.28	0.55	0.85	8.0	238.6	29.8	7.37
0.700	0.36	0.76	0.81	7.8	161.1	20.6	7.08
0.900	0.44	0.85	0.78	8.7	119.5	13.7	5.15
1.100	0.51	0.86	0.76	10.4	93.9	9.1	3.39
1.300	0.58	0.81	0.74	13.0	75.2	5.8	2.06
1.500	0.67	0.73	0.71	17.0	61.0	3.6	1.18
1.700	0.74	0.62	0.70	22.8	51.2	2.2	0.64
1.900	0.81	0.45	0.68	35.0	44.3	1.3	0.27
2.100	0.88	0.16	0.67	106.4	39.2	0.4	0.03

Figure 4 (upper panel) displays the dependence of pairing gaps on baryon density for the composition of matter implied by our chosen EoS. (Note that gaps displayed in Fig. 3 as functions of Fermi momenta of particles are EoS independent, whereas those in Fig. 4 are specific to our EoS.) The dependence of the H_{c2} field on density is shown in Fig. 4 (lower panel). It is seen that magnetars with interior fields with $B \leqslant \max H_{c2} \simeq 7.37 \times 10^{16}$ G will be partially superconducting, which means that regions where $B < H_{c2}$ will be superconducting whereas the regions where $B > H_{c2}$

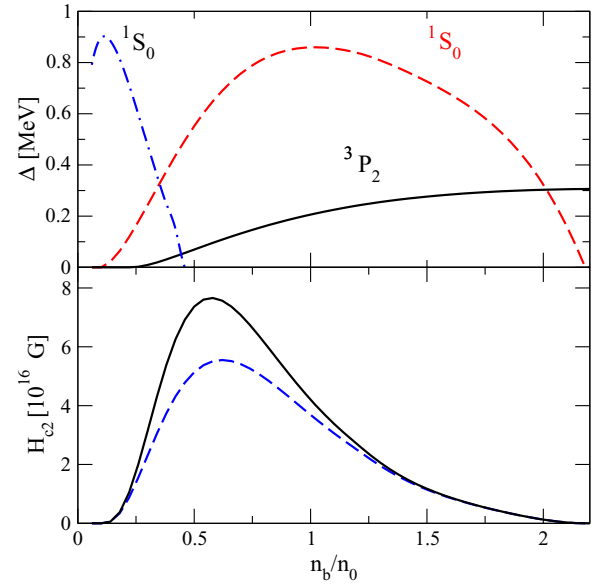

FIG. 4. (Color online) Upper panel: Dependence of pairing gaps for neutrons ($^1S_0$ and $^3P_2$ channels) and for protons ($^1S_0$ channel) on baryonic density in units of nuclear saturation density. Lower panel: Dependence of the critical unpairing field H_{c2} on baryonic density with account for the coupling between the neutron and proton condensates (full line) and without (dashed line).

are not. Clearly, magnetars with $B > \max H_{c2}$ will be fully non-superconducting. The maximum of H_{c2} is attained close to the crust-core interface (corresponding to $n_b = 0.5n_0$). This implies that for partially superconducting magnetars with $B < \max H_{c2}$ the unpairing by the magnetic field will remove proton superconductivity in the inner core, whereas the outer core could be still superconducting provided the B field is approximately homogeneous and constant in the fluid core of the star. This is a reasonable assumption, because the density gradients are small in the fluid core.

IV. NEUTRINO EMISSIVITY OF MAGNETAR CORES

This section studies the implications of the unpairing effect, discussed in the previous section, on the neutrino emission processes from dense matter in magnetars. We focus below on the neutrino emission processes which are dominant below the critical temperature T_{cp} of proton superconductivity, specifically the B-field assisted Urca and the pair-breaking processes. The implications of the unpairing effect for processes such as the modified Urca process and the modified bremsstrahlung process are analogous to those for the direct Urca process and the implementations in numerical codes should be straightforward.

A. Direct Urca process

The direct Urca process is kinematically allowed only above the threshold $Y_{\rm Urca} = n_p/n_b > 11\%$ in ordinary low-field compact stars, because for low proton concentrations the energy and momentum conservation cannot be fulfilled simultaneously [14]. Strong B fields change the phase-space of baryons. As a consequence, the direct Urca process is allowed even below the threshold $Y_{\rm Urca}$ [15,16]. To characterize the kinematics of the Urca process in a B field it is convenient to introduce the parameter [16]

$$x = \frac{k_{Fn}^2 - \left(k_{Fe} + k_{Fp}\right)^2}{k_{Fn}^2} N_{Fp}^{2/3}, \tag{16}$$

where $N_{Fp} = k_{Fp}^2/2|e|B$ is the number of Landau levels populated by protons. Thus, for $x > 0$ the Urca process is forbidden in the low-field limit, but can become operative in strong magnetic fields.

If, under such conditions, the Urca process operates at a fraction of its strength, it can still be an important factor in cooling the star's core, because other processes are by orders of magnitude weaker. For $x < 0$ the Urca process is allowed and the role of the magnetic field is to induce "de Haas–van Alfven" type oscillations in the emissivity of this process as a function of B field.

The second effect of the strong magnetic field on the Urca process (not discussed so far) is the effect of unpairing of the proton superconductor by the field. Proton and neutron pairings restrict the phase space available for the process and, as a consequence, the rate of the direct Urca process is suppressed. This suppression at asymptotically low temperatures is given simply by an exponential quenching factor $\exp(-\Delta/T)$ for each participating nucleon, where Δ is the relevant pairing gap, T is the temperature (more accurate treatments are given, e.g., in Ref. [17]). As outlined in Sec. III, large B fields unpair the proton superconductor, therefore the suppression of the Urca neutrino emission due to the gap in proton quasiparticle spectrum will be absent, i.e., only neutron pairing will contribute to the suppression. Because the gap for neutrons in the P-wave channel is smaller than the one in the S-wave channel for protons (see Fig. 4), the onset of suppression will strongly deviate from the one expected in the case of superconducting protons.

We now illustrate these qualitative arguments by numerical examples. In our setup the proton fraction remains below $Y_{\rm Urca}$ in the density range where proton S-wave superconductivity exists, i.e., densities $n \leqslant 3n_0$, therefore we explore first the domain $x > 0$, where Urca process is forbidden in the zero-field limit. The Urca emissivity for $B \neq 0$ is written as [16]

$$\epsilon^{\rm Urca} = \frac{457\pi G_F^2}{10080}\left(1 + 3g_A^2\right) m_n^* m_p^* \mu_e T^6 \mathcal{R}\mathcal{S}_n\mathcal{S}_p. \tag{17}$$

where G_F is the Fermi coupling constant, g_A is the axial-vector coupling, $m_{n/p}^*$ are the effective masses of neutron and proton, μ_e is the chemical potential of electrons, $\mathcal{R}$ function encodes modifications due to the field and $\mathcal{S}_{n/p} = \exp(-\Delta_{n/p}/T)$ are the suppression factors arising owing to the pairing of neutrons (n) and protons (p). The quenching of proton superconductivity implies $\mathcal{S}_p = 1$ in Eq. (17). To model the function $\mathcal{R}$ in the forbidden region we use an approximate polynomial fit to the functions shown in Fig. 1 of Ref. [16], which is given by $\log_{10}\mathcal{R} = -0.35942 - 0.506418x + 0.0130305x^2 - 0.00140399x^3$. In the allowed domain we use the fit formula [16]

$$\mathcal{R} = 1 - \frac{\cos\phi}{0.5816 + |x|^{1.192}}, \tag{18}$$

where $\phi \equiv (1.211 + 0.4823|x| + 0.8453|x|^{2.533})/(1 + 1.438|x|^{1.209})$ which is valid in the range $-20 \leqslant x \leqslant 0$ and $N_{Fp} \to \infty$. Figure 5 displays the neutrino emissivity via the Urca process in the forbidden region as a function of the B field at fixed density ($n = n_0$) and two values of temperature. The unpaired case coincides with the results of Refs. [15,16]. Magnetic field allows the Urca process to operate with emissivity comparable with the emissivities of competing processes in the asymptotically large field region $B \to B_{\rm max}$, as seen in Fig. 5. The pairing of neutrons and protons requires an additional multiplicative factor $\mathcal{S}_n\mathcal{S}_p = \exp[-(\Delta_n + \Delta_p)/T]$ in the neutrino emissivity. We show the cases $\Delta_p = 0$ and $\Delta_p \neq 0$ assuming that the neutron pairing gap $\Delta_n \neq 0$ and corresponds to its value at $B = 0$. Because for all B-field values $B > \max H_{c2}$ ($\log_{10}[\max H_{c2}] = 16.87$) the unpairing effect requires $\Delta_p = 0$; thus the case $\Delta_p \neq 0$ is not realized physically, but provides a measure of the error of neglecting the unpairing effect. It is evident from Fig. 5 that this error is substantial and is the consequence of the fact that $\Delta_p \gg \Delta_n$ in our example. This condition holds except at the edge of the density domain of interest, see Fig. 4. Thus, the proton pairing, if allowed, would suppress the emissivity stronger than the neutron pairing, but because of the unpairing effect the Urca emissivity is suppressed by the neutron superfluidity only.

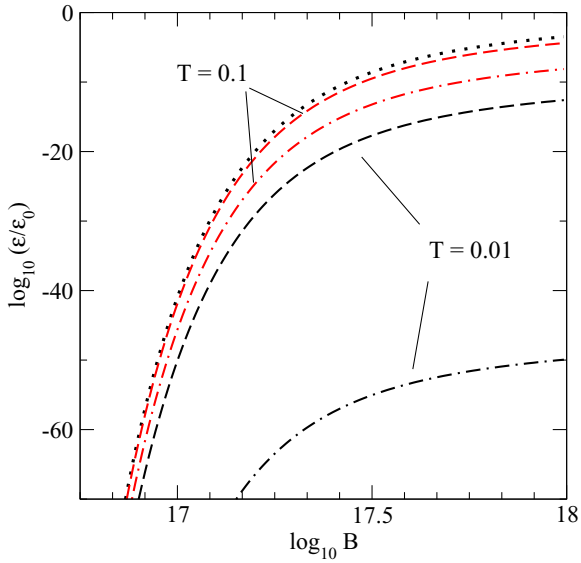

FIG. 5. (Color online) The emissivity of the Urca process in the forbidden region ($x > 0$) in units of the zero-field emissivity ϵ_0 at fixed density $n = n_0$ for temperatures $T = 0.01$ and 0.1 MeV. The Urca emissivity is shown for the cases of (a) normal matter (dotted line), (b) paired neutrons and normal protons (dashed lines), and (c) paired neutrons and protons (dashed-dotted lines). However the case (c) cannot be realized because of the unpairing effect for all the plotted values of $B > H_{c2} = 16.57$. Note that for fixed density the scaling of the kinematical factor x along the B axis is given through its dependence on the number of Landau levels, i.e., $x \propto N_{Fp}^{2/3} \propto B^{-2/3}$.

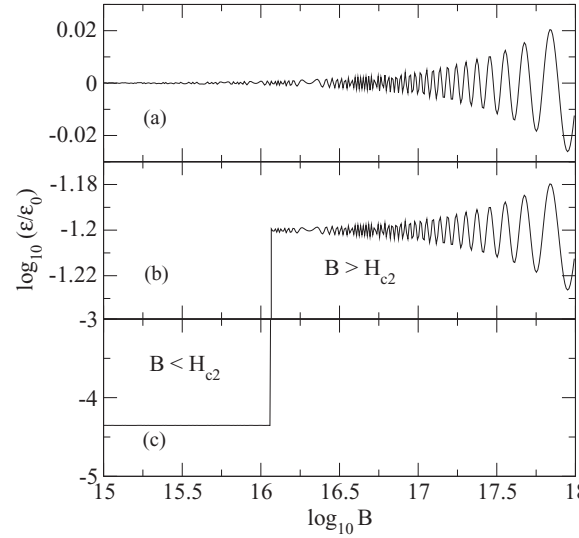

FIG. 6. The emissivity of the Urca process in the allowed region ($x < 0$) in units of the zero-field emissivity ϵ_0 at fixed density $n = 1.5\,n_0$ for temperature $T = 0.1$ MeV. The magnitude of proton and neutron gaps are $\Delta_p = 0.73$ MeV and $\Delta_n = 0.28$ MeV. The emissivity is shown in the cases of (a) unpaired matter, (b) paired neutrons and for $B > H_{c2}$ (unpaired protons), and (c) paired neutrons and for $B < H_{c2}$ (paired protons).

As a consequence the Urca emissivity would be enhanced from its value which neglects the unpairing effect. To explore the allowed region $x \leqslant 0$ of kinematics for the Urca process in a strong magnetic field we have artificially increased the Fermi momenta of protons and electrons by factor of two. (In our models the proton fraction exceeds the Urca threshold at density which is larger than the maximal density at which proton S-wave superconductivity exists.) We also choose to work at density $1.5\,n_0$ because the Urca process becomes operative in the high density domain. Figure 6 displays the neutrino emissivity of the Urca process in the allowed region as a function of the B field for unpaired matter and for cases $B < H_{c2}$ (superconducting protons) and $B > H_{c2}$ (non-superconducting protons). In the case of unpaired neutrons and protons [Fig. 6(a)], the B field induces de Haas–van Alfven type oscillations in the emissivity around its value in the zero B-field limit, as expected [15,16]. For fields $B < H_{c2}$ the emissivity is suppressed by neutron and proton pairing simultaneously; for $B > H_{c2}$ protons are unpaired and the suppression is only due to paired neutrons. The transition from one regime to the other is seen as a jump in the emissivity in (b) and (c) of Fig. 6 at $B = H_{c2}$. The oscillations in (b) are around a value of emissivity which is about an order of magnitude smaller than the emissivity in the normal state, which reflects the suppression via neutron pairing only. If the unpairing effect was neglected the emissivity would have remained about 4–5 orders of magnitude below $B = 0$ case. Strong magnetic fields will influence the neutron superfluidity in the curst (S wave) and in the core (P wave) differently. The S-wave condensate forms spin-zero Cooper pairs and the Pauli paramagnetic alignment of neutron spins along the B field will act to quench their pairing. Generally, this quenching is effective for fields larger than those discussed here ($B > 10^{17}$ G), but the value of the critical field depends on the gap in the zero field limit, which has an uncertainty of an order of magnitude. The P-wave condensate forms spin-one Cooper pairs and the magnetic field will align the spins of Cooper pairs without affecting their internal structure. Initial studies of P-wave pairing in strong fields show that there is no suppression of the pairing induced by the field [18]. Therefore, as far as the Urca process is concerned, we do not expect additional suppression of pairing due to the B field in the P-wave paired core.

Thus we conclude that the unpairing effect which destroys the proton condensate can strongly influence the neutrino emissivity via the Urca process in the cores of magnetars. These modifications may have important consequences on the modeling of thermal transients and cooling in magnetars.

There exists an additional channel of neutrino losses, which arises once the interaction energy of the B field with the spin of a nucleon becomes of the order of temperature—the direct bremsstrahlung process $N \to N + \nu + \bar{\nu}$, where N refers to a nucleon. This process is strictly forbidden in the nonmagnetic case, but becomes operative in a strong enough B field, because of the paramagnetic splitting of the energies of nucleons in a strong B field. Spin-flip neutrino emission is effective within the window of splitting energies of the order of the temperature of ambient matter [19]. By the same argument as in the case of the Urca process above, the bremsstrahlung process $p \to p + \nu + \bar{\nu}$ will remain intact in magnetars, in contrast to the

case of ordinary neutron stars, where it would be suppressed by the proton pairing at low enough temperatures.

B. Pair-breaking processes

The formation of nucleonic BCS condensates leads to the pair-breaking neutrino emission from each nucleonic condensate [20–24]. In this subsection we study how the unpairing effect changes the neutrino emissivity if the B field exceeds the critical value H_{c2} locally. To quantify the pair-breaking neutrino emission, consider their neutrino emissivity, which is given by ($\hbar = c = 1$, our notations follow Ref. [25])

$$\epsilon_n = \frac{4G_F^2 m_n^* k_{Fn}}{15\pi^5} T^7 a_n^{S/P} \left(\frac{\Delta_n^{S/P}}{T}\right)^2 \mathcal{I}, \tag{19}$$

$$\epsilon_p = \frac{4G_F^2 m_p^* k_{Fp}}{15\pi^5} T^7 a_p^{S} \left(\frac{\Delta_p}{T}\right)^2 \mathcal{I}, \tag{20}$$

where the subscripts n and p refer to neutrons and protons and the superscripts S and P refer to $^1S_0$ and $^3P_2$ pairing of neutrons. Δ_n^P in Eq. (19) stands for the angle averaged value of the spin-triplet neutron gap, in which case it can be factored out of the integral $\mathcal{I}$. (The explicit form of the integral $\mathcal{I}$ is not needed here and can be found, for example, in Ref. [25]). The a coefficients are defined as

$$a_n(^1S_0) = \frac{4}{81} c_{nV}^2 v_{Fn}^4 + \frac{11}{42} c_{nA}^2 v_{Fn}^2 \chi_n, \tag{21}$$

$$a_p(^1S_0) = \frac{4}{81} c_{pV}^2 v_{Fp}^4 + \frac{11}{42} c_{pA}^2 v_{Fp}^2 \chi_p, \tag{22}$$

$$a_n(^3P_2) = \frac{c_{nA}^2}{2}, \tag{23}$$

where $\chi_{n/p} = 1 + (42/11)(m_{n/p}^*/m_{n/p})^2$, $c_{nV} = 1$, $C_{nA} = g_A$, $C_{pV} = 4\sin^2_W - 1$, and $C_{pA} = g_A$, with $g_A \simeq 1.26$ and $\sin^2\theta_W = 0.23$.

Figure 7 displays the functions

$$Q_{n/p}(B)[\mathrm{fm}^{-1}] = \frac{m_{n/p}^* k_{Fn/Fp}}{m_{n/p}} a_{n/p}^{S/P} \left(\frac{\Delta_n^{S/P}}{T}\right)^2, \tag{24}$$

which are more convenient for our analysis than the emissivities as all common factors appearing in the emissivities (19) and (20) are discarded (including the temperature, which is assumed to be constant throughout the core and the inner crust of the star). In the crust of the star (i.e., for densities $n \leqslant 0.5 n_0$) the pair-breaking emission is due to the $^1S_0$ paired neutron Cooper pairs. This process is unaffected by the unpairing effect and is shown for comparison. At larger densities, in the core of the star, neutron and proton Cooper pair-breaking processes contribute about equally to the neutrino energy loss in the zero-field limit [Fig. 7(a)]. The influence of the unpairing effect is seen in (b) and (c) where we assume constant value of the field $B_{16} = 5 \times 10^{15}$ and $B_{16} = 10^{16}$ G. The constant B field removes the proton pair-breaking processes in the regions where $B > H_{c2}$ locally, because the condensate vanishes in that region. As a consequence the total emission rate is reduced to its value corresponding to the emission by the P-wave condensate.

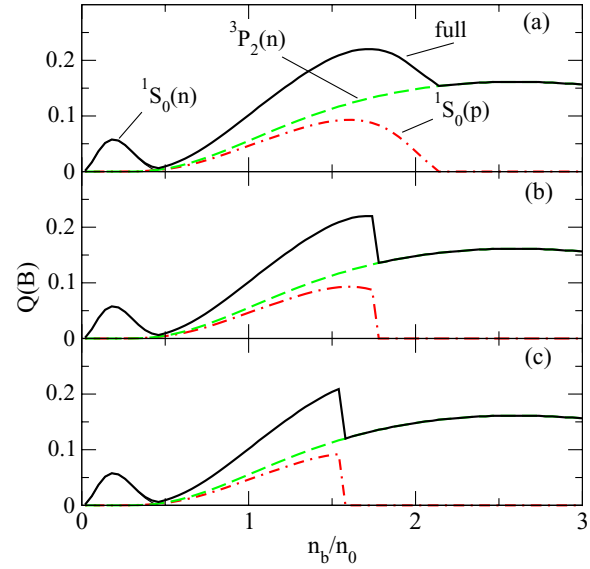

FIG. 7. (Color online) Neutrino emissivity via pair-breaking processes as a function of baryon density in units of n_0 for $B_{16} = 0$ (a), $B_{16} = 0.5$ (b), and $B_{16} = 1$ (c). The full pair-breaking emissivity is shown by solid lines and consists of $^1S_0$ neutron pair emission for $n_b/n_0 > 0.5$ and of the sum of $^1S_0$ proton and $^3P_2$ neutron pair emission for larger densities. The separate contributions of $^1S_0$ proton and $^3P_2$ neutron pairs are shown by dash-dotted and dashed lines, respectively.

The unpairing effect will influence, apart from the emissivities of the magnetars, also their thermal inertia, because the absence of proton superconductivity will enhance the heat capacity of the star. As a consequence the timescale needed for the star's temperature to reach a given value will be larger than in the case of absence of unpairing. In superconducting stars the main source of heat capacity are electrons; in magnetars non-superconducting protons will approximately double the heat capacity of the core of the star. Thus, we anticipate that the proton and electron specific heats decrease linearly with temperature as in normal Fermi liquids, whereas the heat capacity of superfluid neutrons will be reduced by their superfluidity (exponentially in the case of S-wave pairing and as power-law in the case of P-wave pairing). The unpairing induced reduction of the neutrino emissivity and the increase of the specific heat of matter will both act to increase the cooling time-scale of the star.

C. Relating the surface and crust-core boundary B fields

Because only the surface $B_s \simeq 10^{15}$ G fields are observed in magnetars it appears to us useful to address the problem of relating these observed surface fields to those in magnetar interiors as predicted by theoretical models. Equilibria of magnetized neutron stars with superconducting cores have been constructed in Refs. [26,27]. Both poloidal and toroidal fields, as well as their combinations have been considered. These studies suggest a linear relation of the form

$$B_s \simeq \alpha_B H_b, \tag{25}$$

where H_b is the field intensity at the outer boundary of the core and B_s is the surface field. For purely poloidal field Ref. [26] finds $\alpha_B = \epsilon_b/3$ where $\epsilon_b R$ is the thickness of the crust, R being the radius of the star. This relation was derived for low fields $B \sim H_{c1}$, where the role of the lattice of flux tubes can be neglected and these can be treated as isolated entities. Its validity for larger fields $B \sim H_{c2}$, more relevant to our discussion of the unpairing effect, is not known. Nevertheless, we extracted the values of ϵ_b using our EoS shown in Sec. II assuming that the crust-core boundary is at $n \simeq 0.5 n_0$. We find that there is roughly two orders of magnitude drop in the field value between the crust-core boundary and the surface of the star. Specifically, for the 1.4 $M_\odot$ star model $\alpha_B = 0.058$ and for the 2.67 $M_\odot$ star model $\alpha_B = 0.021$ [28]. The study of Ref. [27], which uses a different method, suggests that the drop of the field from the magnetic pole to the base of the crust is smaller and in the limit of large fields is of order of unity. Clearly, further work is needed to establish the relation (25) in the strong-field regime $B \sim H_{c2}$. While the relation (25) is highly important for relating the physics of the unpairing effect to the observations of magnetars, our discussion and results are independent of the value of the coefficient α_B appearing in that relation.

V. SUMMARY AND OUTLOOK

We have calculated the critical field H_{c2} for unpairing for the proton condensate, including its coupling to the density of the background neutron condensate, using Ginzburg-Landau theory in the vicinity of superconducting-normal phase transition. We find that this coupling enhances the value of the critical field by $\simeq$30% (Fig. 4).

The composition of dense matter and the dependence of proton pairing gap on the Fermi momentum implies that the coherence length has a minimum as a function of density which translate into a maximum in the critical field (see Table I). The maximum is at the crust-core boundary and the critical field decreases towards the center of the star. Assuming the homogeneous constant B field across the core and the inner crust of the star, implies that magnetars with interior fields $B < \max H_{c2}$ are partially non-superconducting, whereas magnetars with $B > \max H_{c2}$ are void of proton superconductivity.

The unpairing effect implies that the emissivity of the direct Urca process is only Boltzmann-suppressed due to neutron gap and therefore is more efficient than its counterpart in low-field matter, where there is an additional suppression due to proton pairing (see Figs. 5 and 6, which illustrate the argument in the allowed and forbidden kinematical domains, respectively). Unpairing further implies that the Cooper pair-breaking processes in protonic matter are absent; this reduces the local net pair-breaking emissivity of matter by a factor of a few (see Fig. 7). In addition unpairing increases the specific heat of magnetar cores and, therefore, the thermal inertia of the core by a factor of two. Combined, the decrease in pair-breaking neutrino emissivity and the increase of the specific heat will increase the cooling time-scale of the star. This would be counterbalanced by enhancement in the direct Urca cooling in the strong field limit. Detailed cooling simulations can reveal the relative importance of these different factors in the cooling of magnetars, which we have discussed separately.

It is not possible to state firmly whether the unpairing effect is operative in magnetars with observed surface B fields 10^{15} G or not, because the topology and the strength of the interior fields are not known accurately. If there is an increase of the field from the surface towards the center of the star (say by a factor of 10 to 15), as suggested by a number of studies and broadly conjectured in the literature, then the unpairing effect implies that the observed magnetars are either partially or completely non-superconducting.

A separate issue, to be studied further, is the influence of the strong magnetic fields on the pairing in neutron matter. The S-wave neutron pairing will be suppressed by strong magnetic field due to the Pauli paramagnetic alignment of neutron spins along the B field. The Chandrasekhar-Clogston limiting field for the quenching of S-wave neutron superfluidity is close to the limiting fields compatible with gravitational equilibrium. On the other hand, the P-wave paired neutron fluid does not experience suppression in the B field [18].

ACKNOWLEDGMENTS

The work of M.S. was supported by the Alexander von Humboldt-Stiftung. A.S. was partially supported by a collaborative research grant of the Volkswagen Foundation (Hannover, Germany) and the Deutsche Forschungsgemeinschaft (Grant No. SE 1836/3-1). We are grateful to Mark Alford, John Clark, Nicolas Chamel, Chris Pethick, and Ira Wasserman for helpful feedback on early versions of this work.

APPENDIX: FITTING FORMULAS

The pairing gap for neutrons in the core and the crust and for protons in the core of the star were fitted by suitable functions (a sum of a polynomial and an exponential function) which depend on the Fermi-momenta of respective particles at zero temperature. These are given by

$$\Delta_n({}^1S_0) = 2.76991 - 2.17347/\exp\left(k_{Fn}^2\right) - 5.91497 k_{Fn} + 17.653 k_{Fn}^2 - 19.1544 k_{Fn}^3 + 6.14977 k_{Fn}^4, \quad \text{(A1)}$$

for neutron superfluid in the crusts

$$\Delta_n({}^3P_2) = 5.97989 - 2.45018/\exp\left(k_{Fn}^2\right) - 9.76221 k_{Fn} + 6.24521 k_{Fn}^2 - 1.73691 k_{Fn}^3 + 0.173889 k_{Fn}^4, \quad \text{(A2)}$$

for the neutron superfluid in the core and using the CD Bonn interaction with Bruckner-Hartree-Fock spectrum, and

$$\Delta_p({}^1S_0) = -302.669 + 302.982/\exp\left(k_{Fp}^2\right) - 8.3717 k_{Fp} + 369.944 k_{Fp}^2 - 160.227 k_{Fp}^3 - 11.3246 k_{Fp}^4, \quad \text{(A3)}$$

for the superconducting protons in the core. The effective masses of neutron and protons were assumed to be qual and given by the following fit formula:

$$\frac{m^*}{m} = 1.00661 - 0.649838 k_F + 0.34416 k_F^2 - 0.0441441 k_F^3, \quad \text{(A4)}$$

where k_F stands for neutron or proton Fermi momentum. More accurate treatment would require different effective masses for neutrons and protons, but the corrections to the emissivities are expected to be small, in the range of a few percent.

[1] G. Baym, C. Pethick, and D. Pines, Nature (London) **224**, 674 (1969); P. Muzikar and C. J. Pethick, Phys. Rev. B **24**, 2533 (1981); G. Mendell, Astrophys. J. **380**, 515 (1991); A. D. Sedrakian and D. M. Sedrakian, *ibid.* **447**, 305 (1995).

[2] B. Link, Phys. Rev. Lett. **91**, 101101 (2003); K. B. W. Buckley, M. A. Metlitski, and A. R. Zhitnitsky, *ibid.* **92**, 151102 (2004); Phys. Rev. C **69**, 055803 (2004); D. M. Sedrakian, A. D. Sedrakian, and G. F. Zharkov, Mon. Not. R. Astron. Soc. **290**, 203 (1997); A. Sedrakian, Phys. Rev. D **71**, 083003 (2005); J. Charbonneau and A. Zhitnitsky, Phys. Rev. C **76**, 015801 (2007).

[3] M. Alford, G. Good, and S. Reddy, Phys. Rev. C **72**, 055801 (2005).

[4] G. A. Lalazissis, T. Nikšić, D. Vretenar, and P. Ring, Phys. Rev. C **71**, 024312 (2005).

[5] C. Ducoin, J. Margueron, C. Providência, and I. Vidaña, Phys. Rev. C **83**, 045810 (2011).

[6] G. Colucci and A. Sedrakian, Phys. Rev. C **87**, 055806 (2013); E. N. E. van Dalen, G. Colucci, and A. Sedrakian, Phys. Lett. B **734**, 383 (2014); G. Colucci and A. Sedrakian, J. Phys.: Conf. Series **496**, 012003 (2014).

[7] M. Sinha, B. Mukhopadhyay, and A. Sedrakian, Nucl. Phys. A **898**, 43 (2013).

[8] A. Sedrakian and J. W. Clark, *Nuclear Superconductivity in Compact Stars: BCS Theory and Beyond* (World Scientific Publishing Co, Singapore, 2006), p. 135.

[9] J. Wambach, T. L. Ainsworth, and D. Pines, Nucl. Phys. A **555**, 128 (1993); M. Baldo, Ø. Elgarøy, L. Engvik, M. Hjorth-Jensen, and H.-J. Schulze, Phys. Rev. C **58**, 1921 (1998); M. Baldo, J. Cugnon, A. Lejeune, and U. Lombardo, Nucl. Phys. A **536**, 349 (1992).

[10] T. Alm, G. Röpke, A. Sedrakian, and F. Weber, Nucl. Phys. A **604**, 491 (1996).

[11] D. M. Sedrakyan and K. M. Shakhabasyan, Astrophysics **16**, 417 (1980).

[12] A. F. Andreev and E. P. Bashkin, Sov. J. Exp. Theor. Phys. **42**, 164 (1976); D. M. Sedrakyan and K. M. Shakhabasyan, Sov. Phys. Usp. **34**, 555 (1991).

[13] L. D. Landau and E. M. Lifshitz, *Statistical Pphysics. Pt.2* (Pergamon Press, Oxford, 1980).

[14] J. M. Lattimer, C. J. Pethick, M. Prakash, and P. Haensel, Phys. Rev. Lett. **66**, 2701 (1991); C. J. Pethick, Rev. Mod. Phys. **64**, 1133 (1992); M. Prakash, Phys. Rep. **242**, 297 (1994).

[15] D. Bandyopadhyay, S. Chakrabarty, P. Dey, and S. Pal, Phys. Rev. D **58**, 121301 (1998); L. B. Leinson and A. Pérez, J. High Energy Phys. 09 (1998) 020.

[16] D. A. Baiko and D. G. Yakovlev, Astron. Astrophys. **342**, 192 (1999).

[17] D. G. Yakovlev, K. P. Levenfish, and Y. A. Shibanov, Phys. Usp. **42**, 737 (1999); A. Sedrakian, Prog. Part. Nucl. Phys. **58**, 168 (2007).

[18] A. N. Tarasov, J. Phys.: Conf. Series **400**, 032101 (2012).

[19] E. N. E. van Dalen, A. E. L. Dieperink, A. Sedrakian, and R. G. E. Timmermans, Astron. Astrophys. **360**, 549 (2000).

[20] E. Flowers, M. Ruderman, and P. Sutherland, Astrophys. J. **205**, 541 (1976).

[21] L. B. Leinson and A. Pérez, Phys. Lett. B **638**, 114 (2006).

[22] A. Sedrakian, H. Müther, and P. Schuck, Phys. Rev. C **76**, 055805 (2007); A. Sedrakian, *ibid.* **86**, 025803 (2012).

[23] E. E. Kolomeitsev and D. N. Voskresensky, Phys. Rev. C **77**, 065808 (2008); **81**, 065801 (2010).

[24] A. W. Steiner and S. Reddy, Phys. Rev. C **79**, 015802 (2009).

[25] D. Page, J. M. Lattimer, M. Prakash, and A. W. Steiner, Astrophys. J. **707**, 1131 (2009).

[26] T. Akgün and I. Wasserman, Mon. Not. R. Astron. Soc. **383**, 1551 (2008); K. T. Henriksson and I. Wasserman, *ibid.* **431**, 2986 (2013).

[27] S. K. Lander, Phys. Rev. Lett. **110**, 071101 (2013); Mon. Not. R. Astron. Soc. **437**, 424 (2014).

[28] M. Sinha and A. Sedrakian, arXiv:1403.2829.